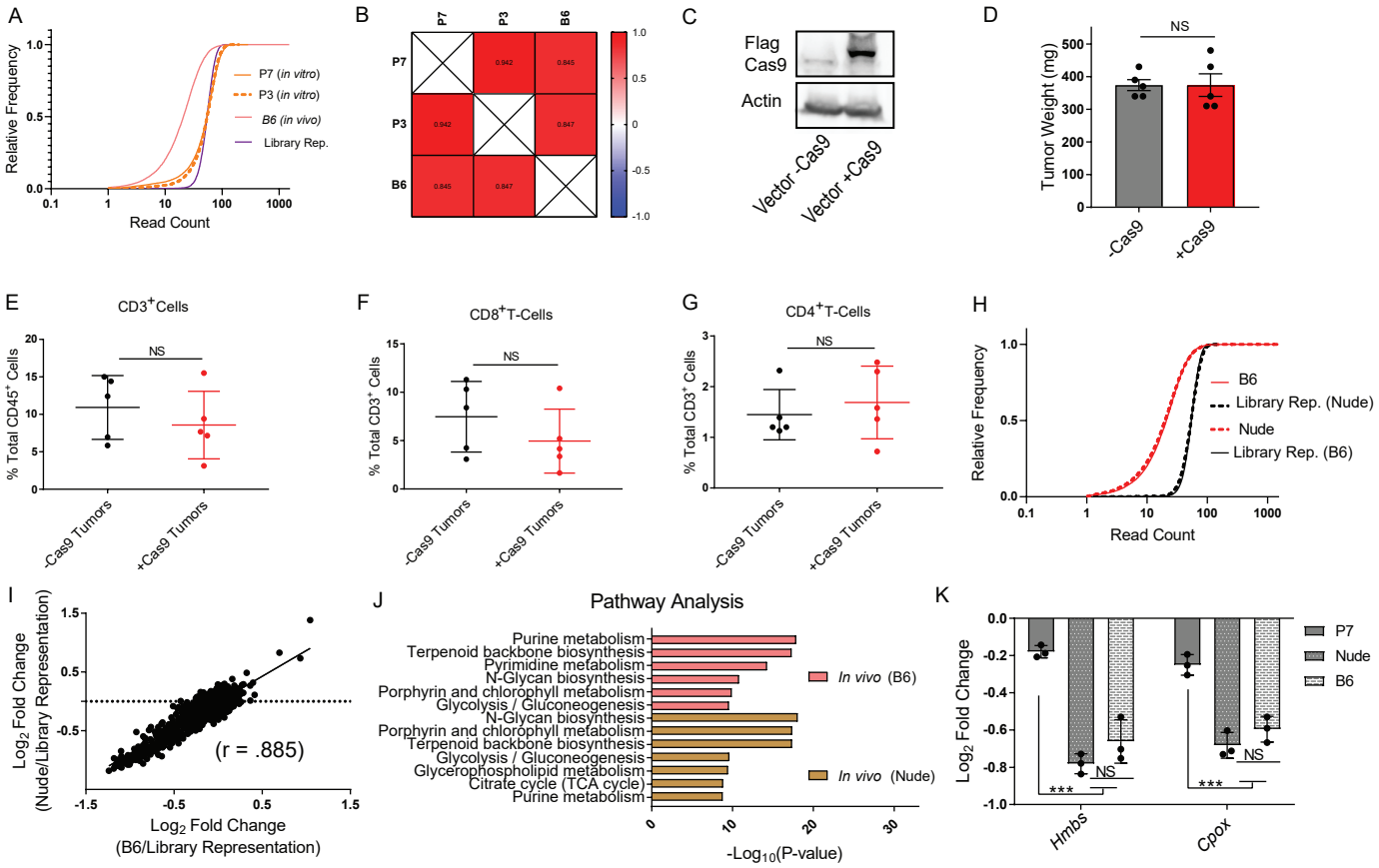

Supplemental Figure 1. Analysis of screen performance (related to Figure 1)

A, Cumulative distribution of sgRNA read counts for the Passage 3 (P3), Passage 7 (P7), and *in vivo* (B6) tumor model experimental conditions along with the corresponding t=0 Library Representation. The $\log_2$(RPM+1) for replicates within experimental conditions are collapsed using the median. **B,** Correlation matrix of normalized log fold changes between the experimental level and the corresponding full representation. Log fold change is calculated for a given condition by subtracting the median log counts from the experimental condition from the corresponding library representation (t=0 after infection/selection). Log fold change is normalized by subtracting out the median log fold change of the negative controls and then dividing by the median log fold change of the positive controls. **C,** Western blot of HY19636 cell lysate for flag tagged spCas9 in cells transduced with plentiCRISPRv2 with or without spCas9. **D,** Tumor weights of HY19636 transduced with plentiCRISPRv2 with or without spCas9 and injected into the flanks of B6 mice. Error bars depict ± s.e.m. of individual tumors. **E,** Quantification of tumor infiltrating CD3+ T-cells as determined by flow cytometry. Error bars depict ± s.d. of whole individual tumors. **F,** Quantification of tumor infiltrating CD8+ T-cells as determined by flow cytometry. Error bars depict ± s.d. of whole individual tumors. **G,** Quantification of tumor infiltrating CD4+ T-cells as determined by flow cytometry. Error bars depict ± s.d. of whole individual tumors. **H,** Cumulative distribution of sgRNA read counts for the *in vivo* tumor model in B6 and Nude mouse experimental conditions along with the corresponding Full Library Representation for each of the conditions. The $\log_2$(RPM+1) for replicates within experimental conditions are collapsed using the median. **I,** Correlation of normalized log fold changes between the in-vivo tumor model in B6 and Nude mouse experimental conditions. Log fold change is calculated for a given condition by subtracting the median log counts from the experimental condition from the corresponding library representation (t = 0 after infection). Log fold change is normalized by subtracting out the median log fold change of the negative controls and then dividing by the median log fold change of the positive controls. Pearson correlation (r) for the comparison of B6 to nude was calculated using the corresponding 95% confidence intervals (0.8767-0.8925). **J,** Pathway analysis of significantly depleted genes (FDR < 0.2) in the immunocompetent (B6) and immunocompromised (nude) hosts using metaboanalyst software. The $-\text{Log}_{10}$ p-value of the most enriched pathways (FDR < 0.005) are plotted. **K,** Log fold change of *Hmbs* and *Cpox* are plotted for P7, Nude, and B6 experimental conditions. Error bars depict ±s.d. of experimental condition (screens were performed in triplicate). For panels b-e and j, significance determined with an unpaired two tailed t-test. *P<0.05, **P<0.01, ***P<0.001, ns: non-significant, P>0.05.

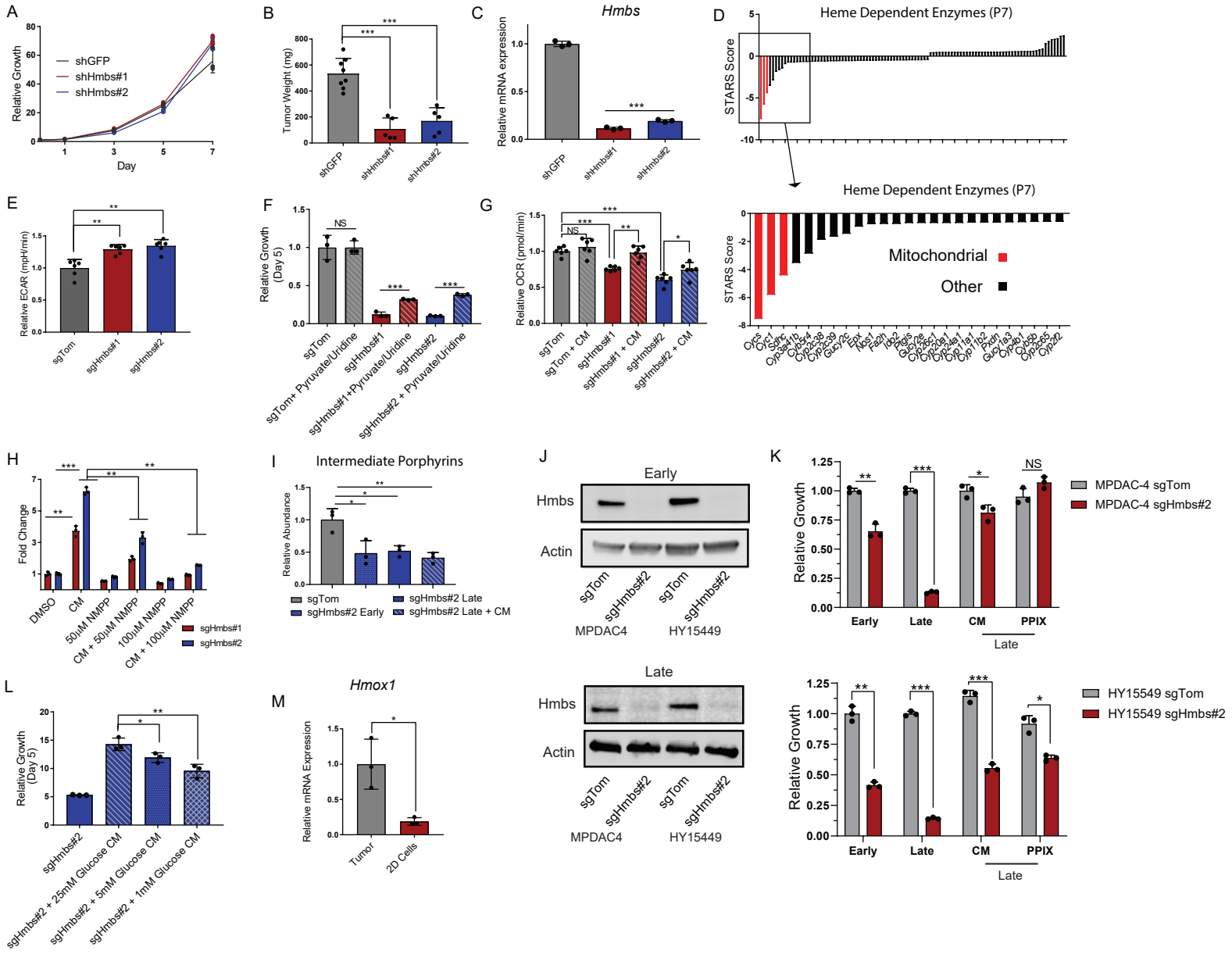

Supplemental Figure 2. Investigating metabolite sharing in pooled screens (related to Figure 2 and 3)

A, Relative proliferation rates of shGFP and shHmbs cells grown in 2D culture and performed after greater than 10 days in 2D culture. Data are plotted as relative cell proliferation normalized to day 0 in arbitrary units. Error bars depict ± s.d. of three independent wells from a representative experiment (of three experiments). **B,** Tumor weight after subcutaneous injection of shGFP (*n* = 8) and shHmbs (KD#1 *n* = 5, KD#2 *n* = 5) cells into the flanks of B6 mice harvested at endpoint. Error bars depict ± s.d. of individual tumor weights. **C,** Relative mRNA expression of *Hmbs* in cells infected with shGFP or shHmbs. Error bars depict ± s.d. of three independent wells. **D,** STARS score of all genes in the library that utilize heme as a co-factor from the passage 7 (P7) screen. Genes that reside in the mitochondria are colored in red whereas all other genes are colored in black. **E,** Relative extracellular acidification rate (ECAR) of late passage sgTom and sgHmbs cells. Data are plotted as relative OCR to sgTom. Error bars depict ± s.d. of six independent wells from a representative experiment (of three experiments). **F,** Relative proliferation rates of late passage sgTom and sgHmbs cells grown in 2D culture. Cells were treated with fresh media or pyruvate and uridine. Data are plotted as relative cell proliferation normalized to day 0 in arbitrary units. Error bars depict ± s.d. of three independent wells from a representative experiment (of three experiments). **G,** Relative OCR of late passage sgTom and sgHmbs cells treated with either fresh media or conditioned media (CM). Data are plotted as relative OCR to media treated sgTom samples. Error bars depict ± s.d of 6 individual wells from a representative experiment (of three experiments). **H,** Fold change of late passage *sgHmbs* cells treated with either DMSO, CM, n-methyl protoporphyrin (NMPP), or NMPP + CM. Assay was performed in 2D culture. Data are plotted as fold change to DMSO treated samples. Error bars depict ± s.d of 3 individual wells from a representative experiment (of three experiments). **I,** Intermediate porphyrin abundance in sgTom cells, early passage sgHmbs cells, late passage sgHmbs cells, or late passage sgHmbs cells treated with CM. Data are plotted as relative abundance to sgTom cells. Error bars depict ± s.d. of three independent samples**. J,** Western blot for Hmbs in MPDAC4 and HY15449 cell lines assesed immediately after selection (early) or after 10 days in culture (late). **K,** Relative growth of early (immediately after selection) and late (> 10 days in culture) passage sgHmbs cells assessed at day 5 after seeding grown in 2D culture. Cells were treated with either fresh media, conditioned media (CM) from sgTom cells, or PPIX. Error bars depict ± s.d. of three independent wells from a representative experiment (of three experiments). **L,** Relative growth of late passage (>10 days in culture) sgHmbs cells treated with either fresh media or conditioned media (CM) from sgTom cells. sgTom cells were grown in full DMEM (25mM glucose), DMEM with 5mM glucose, or DMEM with 1mM glucose to generate CM. Wells were adjusted to 25mM after CM was added to sgHmbs cells. Error bars depict ± s.d. of three independent wells from a representative experiment (of three experiments). **M,** Relative mRNA expression of *Hmox1* in sgTom tumors and 2D cells as determined by RNA sequencing. Error bars depict ± s.d. of three individual tumors or plates of cells. For all panels, significance was determined with an unpaired two tailed t-test. *P<0.05, **P<0.01, ***P<0.001, ns: non-significant, P>0.05.

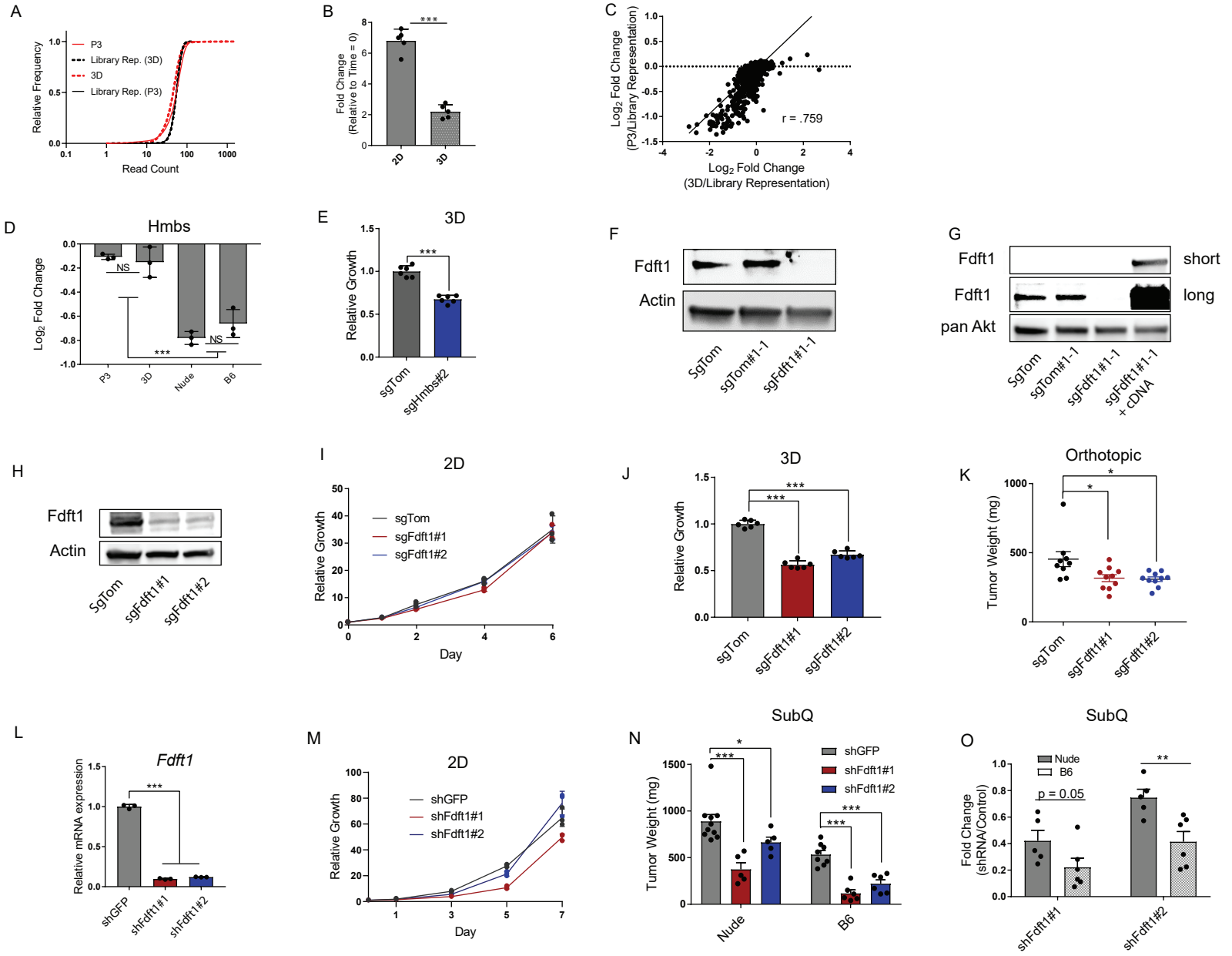

Supplemental Figure 3. 3D metabolic screen reveals requirement of Fdft1 *in vivo* and in 3D culture (related to Figure 3 and 4)

A, Cumulative distribution of sgRNA read counts for the 2D Passage 3 (P3) and 3D experimental conditions along with the corresponding t=0 Library Representation. The $\log_2$(RPM+1) for replicates within experimental conditions are collapsed using the median. **B,** Fold change of cells cultured in either 3D or 2D conditions calculated from seeding density. Error bars depict ± s.d. of cell number measured 48 hours after seeding from a representative experiment. **C,** Correlation of normalized log fold changes between the P3 and 3D experimental conditions. Log fold change is calculated for a given condition by subtracting the median log counts from the experimental condition from the corresponding library representation (t = 0 after infection). Log fold change is normalized by subtracting out the median log fold change of the negative controls and then dividing by the median log fold change of the positive controls. Pearson correlation (r) for the comparison of P3 vs 3D was calculated using the corresponding 95% confidence intervals (0.7345-0.7742). **D,** Log fold change of *Hmbs* is plotted for P3, 3D, Nude, and B6 (Nude and B6 as in Supplemental Data 1K) experimental conditions. Error bars depict ± s.d. of experimental condition (screens were performed in triplicate). **E,** Relative growth of sgTom and sgHmbs cells grown in 3D and assessed by cell titer-glo (CTG). Data are plotted as relative luminescent signal to sgTom. Error bars depict ±s.d. of 6 independent wells from a representative experiment (of three experiments). **F,** Western blot for Fdft1 protein in sgTom (polyclonal), sgTom#1-1 (clone), sgFdft1#1-1 (clone) cell lysates. **G,** Western blot for Fdft1 protein in sgTom (polyclonal), sgTom#1-1 (clone), sgFdft1#1-1 (clone), and sgFdft1#1-1 + *FDFT1* cDNA cell lysates. **H,** Western blot for Fdft1 protein in sgTom, sgFdft1#1, and sgFdft1#2 polyclonal cell lysates. **I,** Relative proliferation rates of sgTom, sgFdft1#1, and sgFdft1#2 polyclonal cells grown in 2D culture. Data are plotted as relative cell proliferation normalized to day 0 in arbitrary units. Error bars depict ± s.d. of three independent wells from a representative experiment (of three experiments). **J,** Relative growth of sgTom, sgFdft1#1, and sgFdft1#2 polyclonal cells grown in 3D culture and assessed by cell titer-glo (CTG). Data are plotted as relative luminescent signal to sgTom. Error bars depict ± s.d. of 6 independent wells from a representative experiment (of three experiments). **K,** Tumor weight after orthotopic implantation of sgTom (n = 9), sgFdft1#1 (n = 10), and sgFdft1#2 (n = 10) polyclonal cells into the pancreata of B6 mice harvested at endpoint. Error bars depict ± s.e.m of individual tumor weights. **L,** Relative mRNA expression of *Fdft1* in cells infected with shGFP or shFdft1. Error bars depict ± s.d. of three independent wells. **M,** Relative proliferation rates of shGFP and shFdft1 cells grown in 2D culture. Data are plotted as relative cell proliferation, normalized to day 0, in arbitrary units. Error bars depict ± s.d. of three independent wells from a representative experiment (of three experiments). **N,** Tumor weight harvested at endpoint from shGFP and shFdft1 cells injected into the flanks of either nude or B6 mice. Error bars depict ± s.e.m of individually weighed tumors. **O,** Fold change of tumors from panel N calculated by dividing shFdft1/shGFP for either the nude or B6 tumors. Error bars depict ± s.e.m of individually weighed tumors. For all panels, significance was determined with an unpaired two tailed t-test. *P<0.05, **P<0.01, ***P<0.001, ns: non-significant, P>0.05.

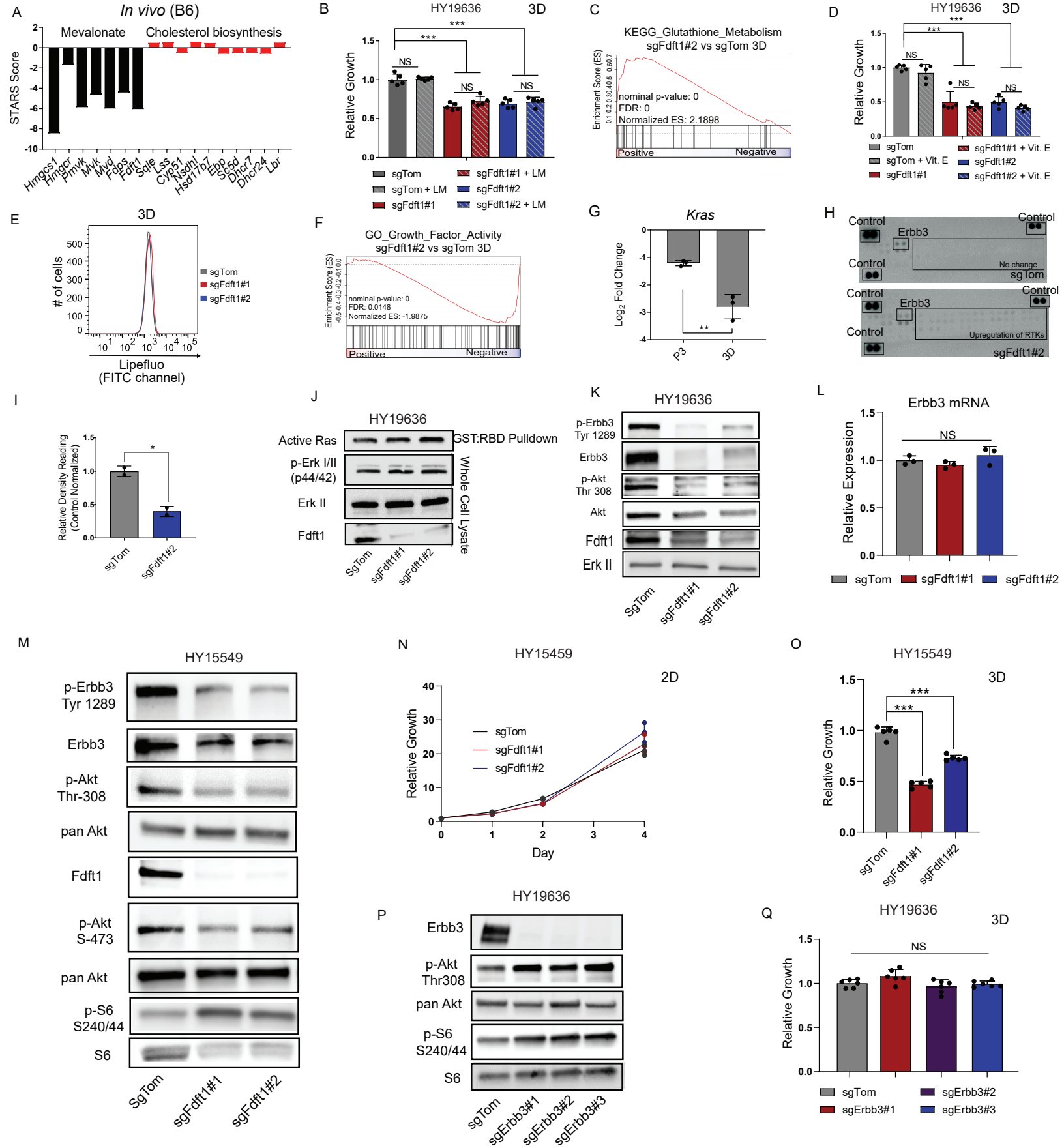
A
In vivo (B6)
Mevalonate
Cholesterol biosynthesis
STARS Score
Hmgcs1
Hmgcr
Pmvk
Mvk
Mvd
Fdps
Fdft1
Sqle
Lss
Cyp51
Nsdhl
Hsd17b7
Ebp
Scs5d
Dhcr7
Dhcr24
Lbr
B
HY19636
3D
Relative Growth
sgTom
sgTom + LM
sgFdft1#1
sgFdft1#1 + LM
sgFdft1#2
sgFdft1#2 + LM
C
KEGG_Glutathione_Metabolism
sgFdft1#2 vs sgTom 3D
nominal p-value: 0
FDR: 0
Normalized ES: 2.1898
Positive
Negative
D
HY19636
3D
Relative Growth
sgTom
sgTom + Vit. E
sgFdft1#1
sgFdft1#1 + Vit. E
sgFdft1#2
sgFdft1#2 + Vit. E
E
3D
# of cells
sgTom
sgFdft1#1
sgFdft1#2
Lipefluo
(FITC channel)
F
GO_Growth_Factor_Activity
sgFdft1#2 vs sgTom 3D
nominal p-value: 0
FDR: 0.0148
Normalized ES: -1.9875
Positive
Negative
G
Kras
Log2 Fold Change
P3
3D
H
Control
Erbb3
No change
sgTom
Upregulation of RTKs
sgFdft1#2
I
Relative Density Reading
(Control Normalized)
sgTom
sgFdft1#2
J
HY19636
Active Ras
GST:RBD Pulldown
p-Erk I/II
(p44/42)
Erk II
Fdft1
Whole Cell Lysate
SgTom
sgFdft1#1
sgFdft1#2
K
HY19636
p-Erbb3
Tyr 1289
Erbb3
p-Akt
Thr 308
Akt
Fdft1
Erk II
SgTom
sgFdft1#1
sgFdft1#2
L
Erbb3 mRNA
Relative Expression
sgTom
sgFdft1#1
sgFdft1#2
M
HY15549
p-Erbb3
Tyr 1289
Erbb3
p-Akt
Thr-308
pan Akt
Fdft1
p-Akt
S-473
pan Akt
p-S6
S240/44
S6
SgTom
sgFdft1#1
sgFdft1#2
N
HY15459
2D
Relative Growth
sgTom
sgFdft1#1
sgFdft1#2
Day
O
HY15549
3D
Relative Growth
sgTom
sgFdft1#1
sgFdft1#2
P
HY19636
Erbb3
p-Akt
Thr308
pan Akt
p-S6
S240/44
S6
sgTom
sgErbb3#1
sgErbb3#2
sgErbb3#3
Q
HY19636
3D
Relative Growth
sgTom
sgErbb3#1
sgErbb3#2
sgErbb3#3

Supplemental Figure 4. The role of Fdft1 in PDA growth (related to Figure 5)

A, STARS score for experimental B6 condition of all genes in the library that make up mevalonate (black) and cholesterol (red) biosythnetic pathways. **B,** Relative luminescence of sgTom and sgFdft1 cells grown in 3D and assessed by cell titer-glo (CTG). Cells were either plated into media or media containing lipid mix (LM). Data are plotted as relative luminescent signal to sgTom. Error bars depict ± s.d. of 5 independent wells from a representative experiment (of three experiments). **C,** Gene set enrichment analysis (GSEA) performed on RNA sequencing data comparing sgTom and sgFdft1#2 cells grown in 3D culture depicting an increase in glutathione metabolism in *Fdft1* KO cells (from 3 independent samples of either sgTom or sgFdft1#2). **D,** Relative growth of sgTom and sgFdft1 cells grown in 3D and assessed by cell titer-glo (CTG). Cells were either plated into media or tocopherol acetate (Vit. E). Data are plotted as relative luminescent signal to sgTom. Error bars depict ± s.d. of 5 independent wells from a representative experiment (of three experiments). **E,** Lipid peroxides in sgTom and sgFdft1 cells as determined by flow cytometry using Liperfluo dye on 3D cultured cells. **F,** Gene set enrichment analysis (GSEA) performed on RNA sequencing data comparing sgTom and sgFdft1#2 cells grown in 3D culture depicting a decrease in growth factor activity in Fdft1 KO cells (from 3 independent samples of either sgTom or sgFdft1#2). **G,** Log fold change of *Kras* is plotted for P3 and 3D experimental conditions. Error bars depict ± s.d. of experimental condition (screens were performed in triplicate). **H,** RTK activation array performed on cell lysate from sgTom or sgFdft1#2 grown in 3D conditions. **I,** Quantification of Erbb3 signal normalized to control signal in panel H. **J,** Western blot of sgTom and sgFdft1 cell lysates for active Ras by GST:Raf1-RBD pulldown, phosphorylated Erk (p-Erk), Erk II, and Fdft1 in whole cell lysate all grown in 3D conditions. **K,** Western blot of sgTom, sgFdft1#1, sgFdft1#2 polyclonal cell lysates for p-Erbb3, Erbb3, Akt1, p-Akt Thr 308, pS6 S240/44, S6, Fdft1, and Erk2 in 3D conditions. **L,** Relative mRNA expression from RNAseq of *Erbb3* in cells infected with either sgTom, sgFdft1#1, sgFdft1#2. Error bars depict ± s.d from 3 independent samples of either sgTom, sgFdft1#1, or sgFdft1#2. **M,** Western blotting of sgTom, sgFdft1#1, sgFdft1#2 polyclonal HY15449 cell lysates for p-Erbb3, Erbb3, p-Akt Thr 308, pan Akt, Fdft1, p-Akt S473, pS6 S240/44, and S6 in 3D conditions. **N,** Relative proliferation rates of sgTom, sgFdft1#1, and sgFdft1#2 polyclonal HY15449 cells grown in 2D culture. Data are plotted as relative cell proliferation normalized to day 0 in arbitrary units. Error bars depict ± s.d. of three independent wells from a representative experiment (of three experiments). **O,** Relative growth of sgTom, sgFdft1#1, and sgFdft1#2 polyclonal HY15449 cells grown in 3D culture and assessed by cell titer-glo (CTG). Data are plotted as relative luminescent signal to sgTom. Error bars depict ± s.d. of 6 independent wells from a representative experiment (of three experiments). **P,** Western blot of sgTom, sgErbb3#1, sgErbb3#2, and sgErbb3#3 polyclonal HY19636 cell lysates for Erbb3, p-Akt Thr 308, pan Akt, pS6 S240/44, and S6 in 3D conditions. **Q,** Relative growth of sgTom, sgErbb3#1, sgErbb3#2, and sgErbb3#3 polyclonal HY19636 cells grown in 3D culture and assessed by cell titer-glo (CTG). Data are plotted as relative luminescent signal to sgTom. Error bars depict ± s.d. of 6 independent wells from a representative experiment (of three experiments). For all panels, significance was determined with an unpaired 2 tailed t-test. *P<0.05, **P<0.01, ***P<0.001, ns: non-significant, P>0.05.

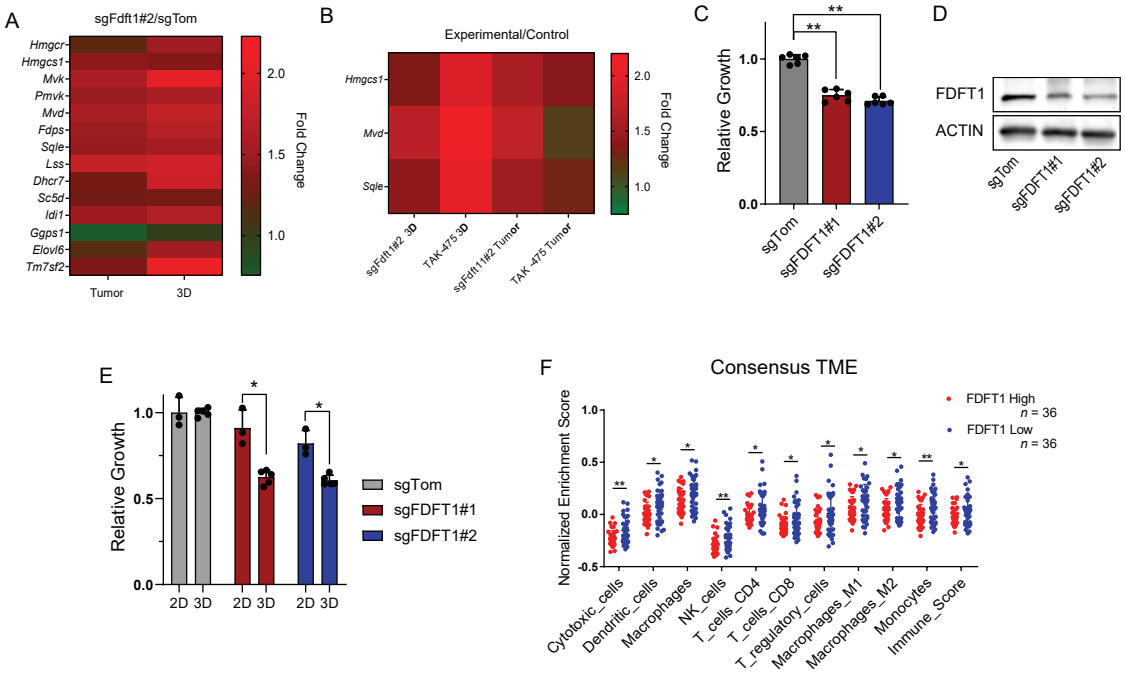

Supplemental Figure 5. Evaluation of FDFT1 as potential therapeutic target (related to Figure 6)

A, RNAseq of fold change of Srebp2 target genes from sgFdft1#2/sgTom cells grown in 3D culture or orthotopic tumors (from 3 independent sample or tumors of either sgTom or sgFdft1#2). **B,** Comparing fold change from subset of Srebp2 target genes in TAK-475 treated tumors/control to RNAseq of sgFdft1#2/sgTom (as in panel A). **C,** Relative growth of human PDA cells MiaPaCa-2 transduced with either sgTom or sgFdft1 and grown in 3D and assessed by cell titer-glo (CTG). Data are plotted as relative luminescent signal to sgTom. Error bars depict ± s.d. of 5 independent wells from a representative experiment (of three experiments). **D,** Western blot for Fdft1 protein levels in *sgTom*, sgFdft1#1, and sgFdft1#2 in MiaPaCa-2 cells lysates. **E,** Relative growth of human Patu-8902 cells transduced with sgTom, sgFdft1#1, or sgFdft1#2. Data are plotted as relative absorbance or luminescent signal to sgTom for 2D and 3D conditions respectively. Error bars depict ± s.d. of 3 or 5 independent wells from a representative experiment for 2D and 3D respectively (of three experiments). **F,** Bulk RNA sequencing from top 20% (high expressing) and bottom 20%(low expressing) of *FDFT1* in PDA patient tumors analyzed by Consensus TME to predict immune cell profiles. (High expressing $n = 36$, Low expressing $n = 36$). For all panels, significance was determined with an unpaired two tailed t-test. *P<0.05, **P<0.01, ***P<0.001, ns: non-significant, P>0.05.

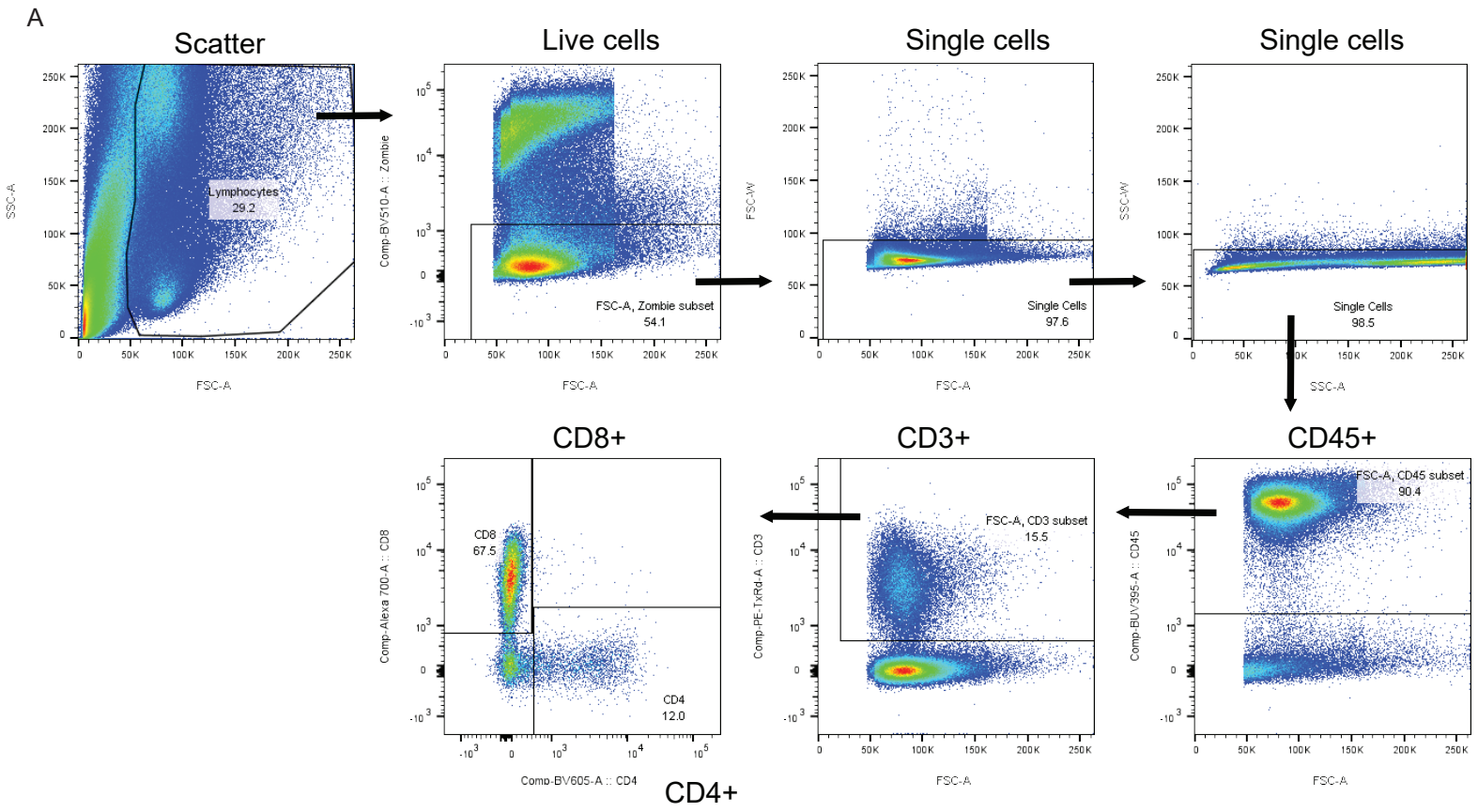

Supplemental Figure 6. Flow cytometry gating strategy (related to Figure S1).

A, Gating strategy used for identifying T-cell populations in tumors trasnduced with or without Cas9 injected into the flanks of B6 mice.